Chapter 2 – Deposition methods

In this chapter the deposition methods used in this study will be discussed in greater detail than in the previous chapter.

2.1 Radio Frequency Plasma Assisted Chemical Vapour Deposition (RF-CVD)

RF-CVD takes place in a vacuum chamber in which there are two electrodes, the powered electrode and the grounded electrode. The powered electrode is where the substrate sits and the grounded electrode usually comprises the chamber outer walls. Process gases are metered in and the pressure is kept constant by means of a number of valves and a vacuum pump removing waste products. RF-Power from a RF-generator is passed between the plates ionising the gas, creating a plasma discharge. It is the ions within the plasma that facilitate the deposition of a film. Therefore an understanding of how the plasma is maintained and the physics within the plasma is essential to understand why thin films are deposited and why they have the properties that they do.

2.1.1 Striking and maintenance of a plasma

In RF-CVD ions are accelerated from a plasma onto the substrate. The plasma is generated by the acceleration of an electron in an applied electrical field. The source of this original electron is either by photoionisation of neutral species by background radiation or by the field emission caused by a strong electric field at a sharp edge in the reactor. As the electron is accelerated it gains energy. When it reaches a high

enough energy it is able to ionise a gas molecule by inelastic collision. This process releases a second electron, which in turn is accelerated in the same fashion. This mixture of ions, electrons and neutrals is the definition of a plasma. Figure 2.1 shows a photograph of a plasma.

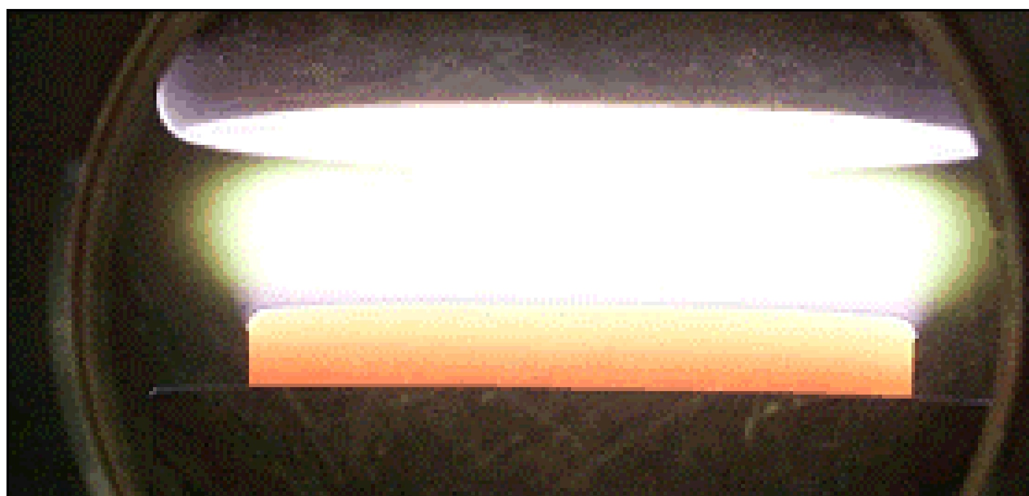

Figure 2.1: A photograph of a plasma[1].

The applied electrical field from the RF generator causes positive ions to be accelerated towards the electrodes. The ions may collide with the electrode (where the substrate is usually placed). Ions may undergo collisions or recombinations with electrons and other ions without colliding with an electrode. Electrons may also collide with chamber walls and be lost. A plasma is only stable if the rate of production of charged particles exceeds the rate of destruction of these charged particles.

The stability of the plasma is a function of many factors including the RF-power, the pressure of the gas within the plasma and the gas mixture.

An increase in the RF-power increases the magnitude of the electrical field and hence the degree of acceleration that charged particles experience and so increases the stability of the plasma. From Equation 2.1 it can be seen that the mean free path (?) of any particle is a function of the speed of the particle ($\bar{c}$). Therefore if the power is too high the electrons' mean free path will increase and the plasma may become unstable (this typically does not happen because the magnitude of the applied electrical field increases causing more electrons to be generated). If the RF-power is too low the electron does not have enough of an accelerating potential to ionise gas molecules.

$$l = \frac{\bar{c}}{z}$$

Equation 2.1: Where l is the mean free path of the particle, $\bar{c}$ is the Root Mean Squared (RMS) velocity of the particle and z is the collision frequency of the particle.

High pressures increase z, this should increase the number of ionisation events which increases plasma stability. But it also increases the number of recombination events and collisions with the chamber electrodes. At low pressures ? is very large and the likelihood of ionisation events decreases.

The ionisation potential of the gas mixture is extremely important, if it is too high it is more difficult to ionise the gas. The mass and size of the gas molecule is also important. If the molecule is large the collision cross-section is increased and if the charged particle has a high mass $\bar{c}$ is lower for the same applied force than a lower mass charged particle, hence ? decreases.

For most gas mixtures a stable plasma can be maintained by finding the optimum values of pressure and RF-Power for that mixture.

2.1.2 The sheath region

In plasmas of the type described above there are at least two regions, the bulk plasma region and the sheath region. Sheath regions surround any surface in the plasma. They are formed due to the large difference in speed between electrons and positive ions in the plasma. Because electrons have a much lower mass and move much more quickly they arrive at the electrode surfaces more quickly than positive ions, and a negatively charged region is formed due to charging at all surfaces (such as electrodes, or the substrate). This negative voltage region grows until it is balanced by electron repulsion. Figure 2.2 illustrates the sheath region. The sheath region does not have as high a concentration of light emitting species as the bulk plasma due to the lower concentrations of electrons in these regions and as a consequence is darker. The sheath region is therefore also known as the 'dark space'.

The potential across the sheath region is very different to that of the bulk plasma. Hence if a positive ion drifts from the bulk plasma region into the sheath region it experiences acceleration towards the surface that the sheath surrounds. The potential between the bulk plasma and the sheath region is known as the sheath potential (V_{sheath}). The potential in the bulk plasma is known as the plasma potential (V_P).

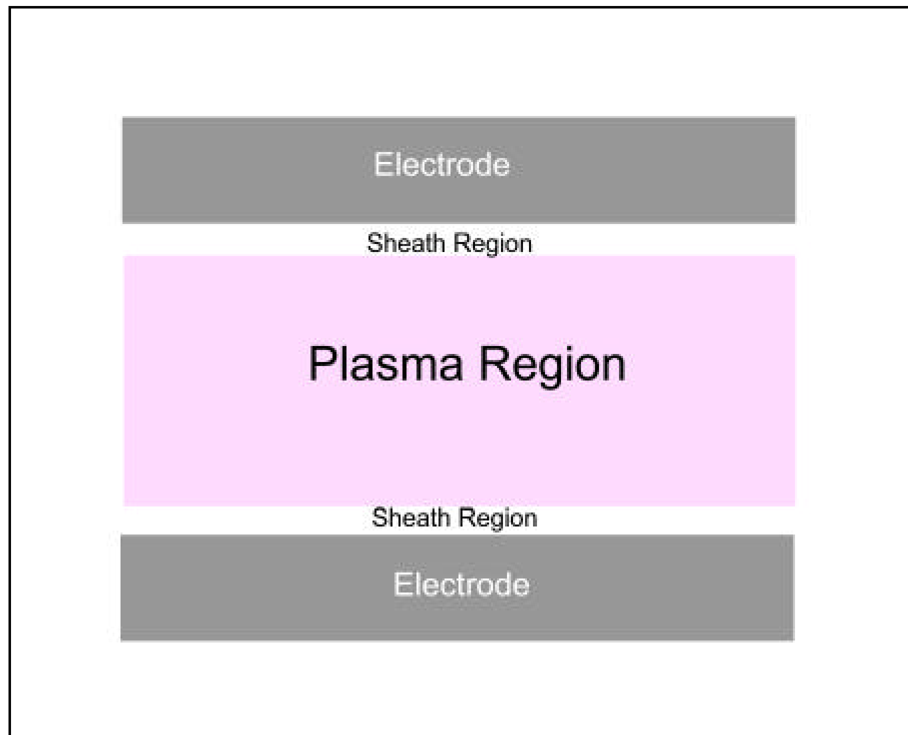

Figure 2.2: Illustration of the regions in a plasma.

2.1.3 DC-Bias

In an RF plasma system the electric field is oscillating at the frequency of the RF-generator. In order to maximise the power going into the plasma the impedance of the RF-generator must equal that of the plasma. Passing the RF-signal through a matching network does this. A matching network consists of a pair of variable capacitors, an inductor coil and several other components. Figure 2.3 shows a typical matching system used for RF plasma deposition systems. An effect of this network is that the net RF current for each cycle must be equal to zero[2].

For plasma reactors with two parallel plates of equal area this requirement is easily satisfied, but if the areas of the electrodes are not the same the sheath potentials around each electrode have to be different to compensate. The DC-Bias (V_{dc}) is the difference in the sheath potentials of the two electrodes. The powered electrode is

usually by design smaller and carries a negative DC-bias. As a consequence the sheath region is larger on the smaller powered electrode, this is shown in Figure 2.4.

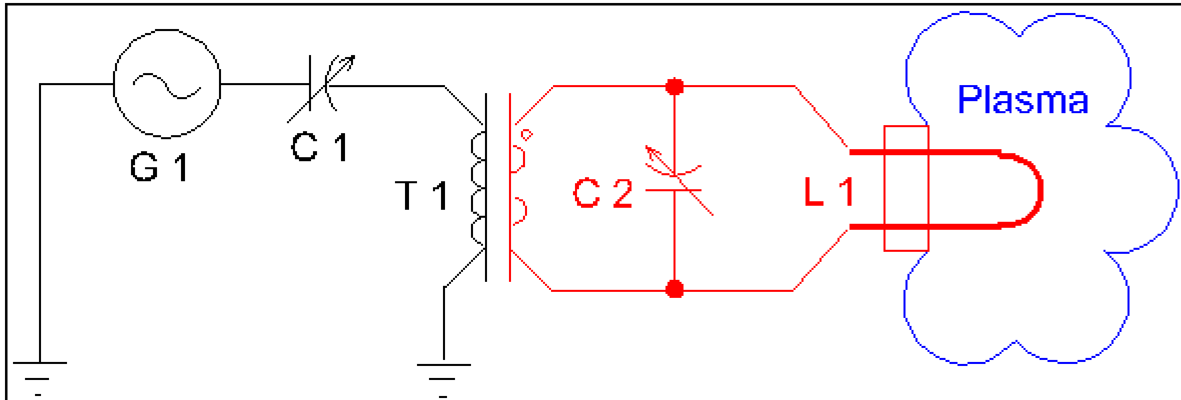

Figure 2.3: A typical RF matching system[3] G1 is the generator C1 and C1 are variable capacitors, T1 is a transformer and L1 is an inductor coil.

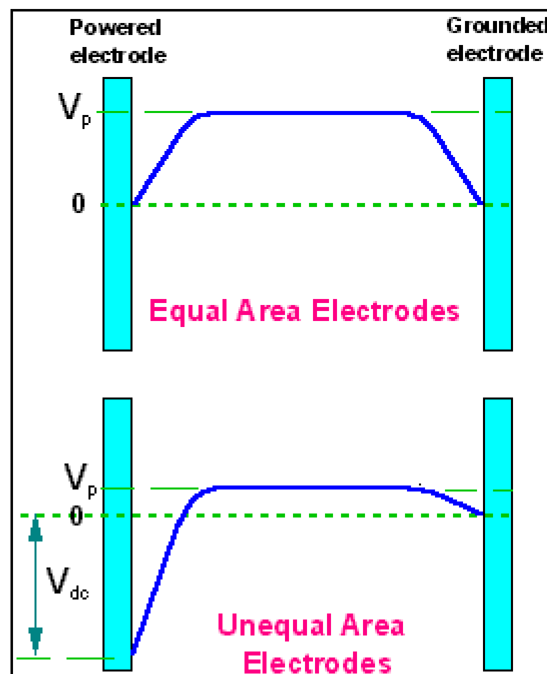

Figure 2.4: Time averaged values for the potentials in different RF-reactors[1].

When a positive ion enters the sheath region near the powered electrode it is accelerated by the potential $V_{dc} + V_p$ towards the powered electrode. As V_{dc} is

typically much larger than V_p, V_{dc} is a good approximation for the potential through which an ion is accelerated.[1]

2.1.4 The Average Ion Energy

The average energy of ions striking the substrate directly affects the properties of the film. So being able to calculate the average ion energy and the spread of energies is important. May *et al*[4-8] have published numerous interesting papers on this work detailing the dynamics of the plasma within the chamber. They calculated the effects of various factors on the average ion energy and the spread of these energies, simulating variations in energy across the sheath. May also completed his PhD using the same deposition chamber as used in this study. He determined that the design of the chamber was such that the DC-Bias gave an approximate value for the average ion energy[5].

Field *et al*[9] introduced a simplified approach to ion energy distributions. In this simplified approach the potential across the sheath region is averaged, which means that it is only a valid model for RF plasmas with frequencies above 10 MHz. The model conveniently gives values for the average ion energy and the spread of the ion energies ($\langle E_{ions} \rangle$ and ? E respectively). They are calculated using V_{dc} and the peak-to-peak voltage ($V_{Pk\text{-}Pk}$) that are usually measured directly from the chamber electrodes. The value $V_{Pk\text{-}Pk}$ is the peak-to-peak voltage of the RF sinusoidal wave that is fed into the reactor by the RF power supply.

$$\langle E_{ions} \rangle = RV_{pe,\max}$$

Equation 2.2

R is the ratio of the area under the $V_{pe}(t)$ curve (the potential curve within the sheath as a function of time) which equates to the average value of the potential mentioned above. R is calculated using the following integral:

$$R = \int_0^{2p} \frac{V_{pe}(t)dt}{[2pV_{pe,\max}]}$$

Equation 2.3

The integral shown in Equation 2.3 does not have an analytical solution, but a table is provided by Field *et al* that directly gives the value of R if the area ratio of the electrodes (A_c/A_A) and V_0 are known (the relationship of V_0 to $V_{\text{pk-pk}}$ is shown in Equation 2.4). V_0 is the amplitude of the sinusoidal wave from the RF-power supply.

$$V_0 = \frac{V_{pk-pk}}{2}$$

Equation 2.4

$V_{\text{pe,max}}$ is the maximum of the potential curve across the sheath and is calculated using:

$$V_{pe,\max} = V_0 - V_{DC} + V_P^O - kT_e \ln(1 + A_c / A_a)$$

Equation 2.5

T_e is the electron temperature and V_P^0 is the floating potential. The floating potential is the potential held by an isolated substrate in the plasma. It is calculated using Equation 2.6.

$$V_P^0 = kT_e \ln(\frac{(kT_e / kT_i)}{\sum \gamma_n \sqrt{(m_e / m_n)}}$$

Equation 2.6

Where T_i is the ion temperature, $?_n$ is the proportion of each process gas, m_e is the mass of one mole of electrons and m_n is the mass of one mole of each ion type.

The electrode area (A_c/A_a) is calculated using Equation 2.7.

$$A_c / A_a = \left(\frac{V_0 + V_{dc}}{V_0 - V_{dc}} \right)^{\frac{2}{\pi}}$$

Equation 2.7

? E, which is the range of ion energies, is calculated using Equation 2.8.

$$\Delta E = \frac{0.899(eV_{pe,\max})^{\frac{3}{2}}}{\pi e f l_{\max} \sqrt{2m_i}}$$

Equation 2.8

e is the charge on an electron, m_i is the average mass of the ions in kg (equivalent to the denominator at the fraction in Equation 2.6) and l_{max} is the maximum height of the sheath on the powered electrode. l_{max} is calculated using Equation 2.9.

$$l_{\max} = 4.93 \times 10^{-5} \left\{ \frac{e\lambda_0}{2m_i} \right\}^{1/5} V_{pe,\max}{}^{3/5}$$

Equation 2.9 [5]

If l_{max} is higher than the mean free path of the ions, the ions are less likely to undergo collisions within the sheath region, thus the scatter of the ion energies will be less, the ion energy distribution (IED) will be similar to that shown in Figure 2.5, there will be two well-defined peaks. The two peaks are due to the phase of the sinusoidal RF

potential when the ion enters the sheath region. If l_{max} is higher than the mean free path of ions in the sheath it is very likely that the ion will collide with a neutral gas molecule, this will reduce the average energy of the IED and cause scatter to occur, hence the IED will be more like a curve, without the two well defined points (Figure 2.6).

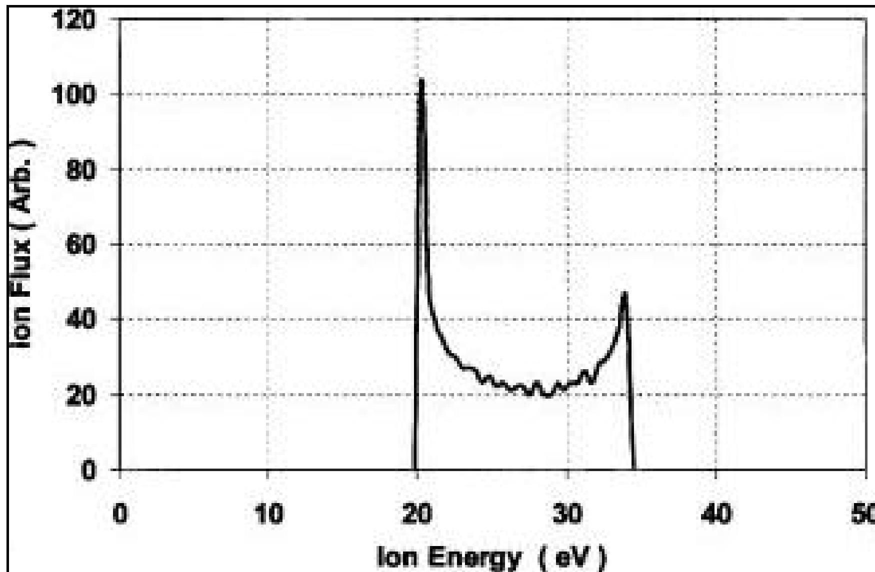

Figure 2.5: The well defined peaks of an ion energy distribution in a low pressure RF-plasma[10].

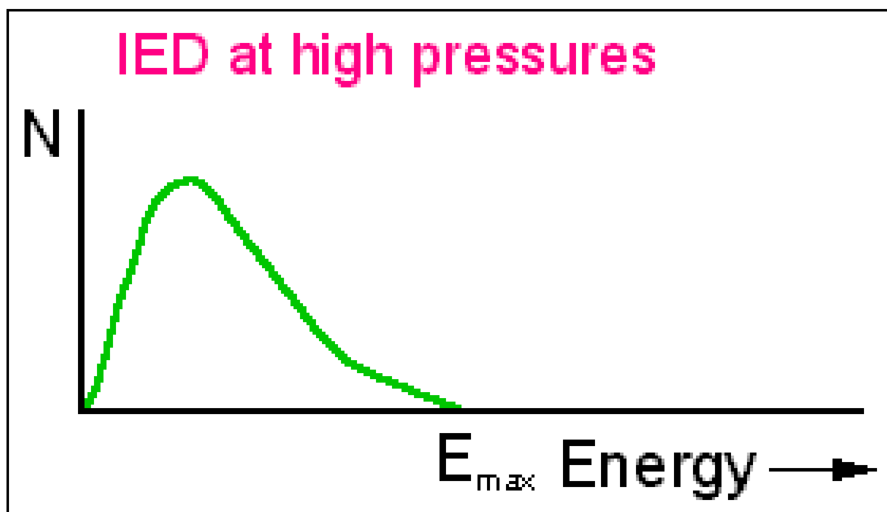

Figure 2.6: The IED at higher pressures, showing the scattering that occurs[1].

In conclusion IEDs are extremely important to know and understand, as they can affect the deposition of thin films. In this study, the plasma conditions will be optimised for both stability and the best film growth.

2.2 Pulsed Laser Ablation at the Solid-Liquid interface.

Pulsed laser ablation (PLA) is a well-known method to produce thin films by ablating material from a solid target of known composition[11]. PLA usually occurs in vacuum, or sometimes in a background of inert gas such as Ar or more reactive gases such as ammonia or nitrogen. Recently a new variation of PLA has been reported whereby the target is immersed in a liquid medium and the laser beam is focused through the liquid onto the target surface[12]. Figure 2.7 shows the setup for this type of experiment.

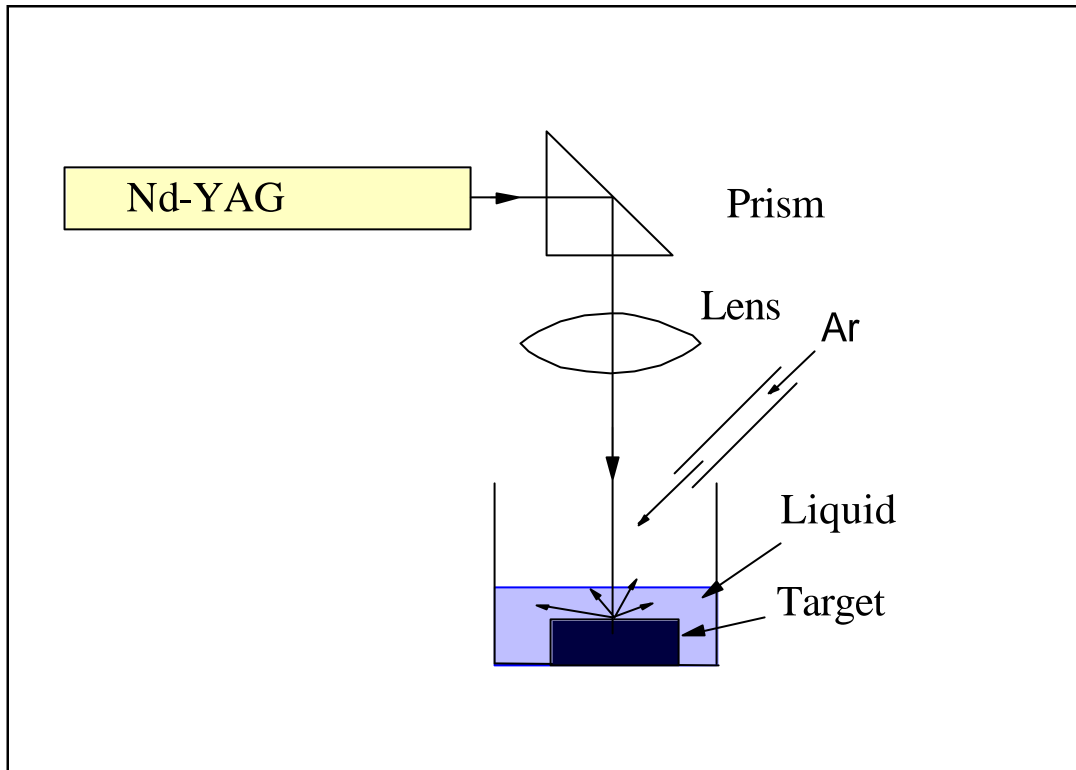

Figure 2.7: The experimental setup for liquid phase pulsed laser ablation.

The interaction of the high intensity laser pulse with the target surface produces an ablation plume of ejected material, in which the surface of the solid target and a small amount of the surrounding liquid are vaporised to form bubbles within the liquid. As more material is vaporised, the bubbles expand, until, at a certain critical combination of temperature and pressure, they collapse[13]. It is believed that when the bubbles collapse the species within are subjected to temperatures of thousands of K and pressures of several GPa and that these extreme conditions allow novel materials to be created[14]. Figure 2.8 shows several images of a laser induced cavitation bubble. This bubble was created at a solid boundary, as it can be seen as time passes the bubble grows larger. It then becomes unstable and collapses. In image (g) the shockwaves from the bubble collapse can be seen.

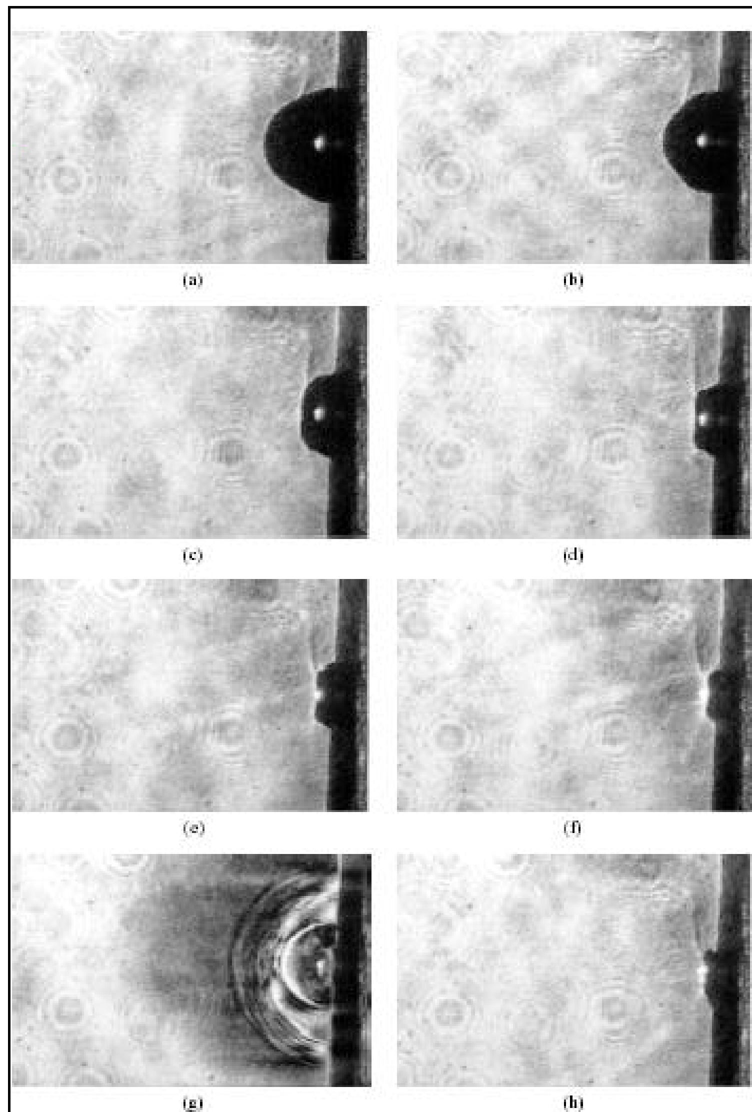

Figure 2.8: images of a single cavitation bubble at a solid boundary, at times (a) 110, (b) 170, (c) 200, (d) 210, (e) 215, (f) 217, (g) 220.5, (h) 224.5 µs after the laser pulse. Taken by Shaw *et al*[13].

The conditions inside these bubbles are similar to cavitation bubbles generated by ultrasonic waves, or by arc discharges under liquids. Ionisation and breakdown of components within the bubbles can occur and the subsequent electron-ion recombination followed by radiative cascade can produce significant optical emission. The advantage of the laser induced cavitation bubble method is that large amounts of a solid target can be vaporised and incorporated into the bubble as well as the liquid, allowing materials to be made which contain a mixture of atoms from the target and the liquid. Unlike the arc discharge method which requires the solid electrode

material to be electrically conducting, the liquid phase PLA method can utilise insulating target materials, allowing a much wider range of novel materials to be produced. The products are usually in the form of nanoparticles that remain suspended within the liquid medium and can be isolated by filtration and evaporation of the liquid.

This novel liquid phase PLA (LP-PLA) technique has been used to produce a variety of materials; Lu and Simakin *et al* produced DLC films from liquid aromatic hydrocarbons and non polar solvents[15,16]. This was done by focusing a KrF laser onto a single crystal Si substrate immersed in the liquid (cyclohexane, benzene or toluene). The Si crystal was covered in DLC. This was identified by laser Raman spectroscopy.

Yang *et al* produced nanocrystals of carbon nitride by ablating graphite in ammonia solution[17]. High resolution transmission electron microscopy (HR-TEM) and selected area electron diffraction (SAED) were used to identify the nanocrystals. SAED identified the cubic crystal phase of carbon nitride.

Dolgaev *et al*[18] produced nanoparticles of Ti, Ag, Au, Si and TiC. This was by ablating the parent metal targets in various liquids. The nanoparticles were identified by TEM and they were found to have a uniform size distribution. When ablating Ti in carbon containing liquids it was found that TiC was formed. They thought that this was due to the breakdown of the liquid and the catalytic nature of the titanium surface. It was proposed that this LP-PLA may be a good way of making many

different types of nanoparticles of materials that have no efficient synthetic route for nanoparticle production.

Recently, Wang *et al.*[19] converted hexagonal boron nitride crystals into cubic boron nitride crystals. The motivation for this was because of cubic boron nitride's extreme properties. It is has properties similar to diamond (high hardness, high thermal conductivity), but unlike diamond it can be deposited on ferrous materials (diamond quickly becomes iron carbide when it is deposited onto ferrous materials) making it a useful material for abrasives and cutting tools. It was produced by the LP-PLA of hexagonal BN under acetone liquid. They presented HR-TEM and powder X-ray diffraction data to support their claim of producing cubic boron nitride.

Nanocrystalline diamond has also been produced by LP-PLA using a graphite target with water or acetone as the liquid medium[20-22]. The authors' main conclusions were that OH groups formed from the oxygen-containing liquids were etching non-diamond carbon species from the surface, thereby allowing diamond to form preferentially. Thus the OH was thought to be playing a role analogous to that of atomic hydrogen in conventional diamond CVD[23].

From the novel materials that have been created, the above work shows that this method may allow for the production of new materials. It is hoped in this study by using LP-PLA as a 'micron sized high pressure high temperature' reactor that crystalline carbon phosphide may be produced and studied.

2.3 References

1 P. W. May, (MSc. Advanced Semiconductor Physics - Plasmas and Plasma Processing - University of Bristol, 1997/1998).

2 B. Chapman, *Glow Discharge Processes*, 1st ed. (John Wiley & Sons, New York, 1980).

3 http://www.casetechnology.com/implanter/rf.html (1998).

4 P. W. May, D. Field, D. F. Klemperer and Y. P. Song, Journal of Physics-Condensed Matter **3,** S257-S264 (1991).

5 P. W. May, PhD Thesis, University of Bristol, 1991.

6 P. W. May, D. Field and D. F. Klemperer, Journal of Applied Physics **71,** 3721-3730 (1992).

7 P. W. May, D. Field and D. F. Klemperer, Journal of Physics D-Applied Physics **26,** 598-606 (1993).

8 P. W. May, D. F. Klemperer and D. Field, Journal of Applied Physics **73,** 1634-1643 (1993).

9 D. Field, D. F. Klemperer, P. W. May and Y. P. Song, Journal of Applied Physics **70,** 82-92 (1991).

10 J. R. Woodworth, I. C. Abraham, M. E. Riley, P. A. Miller, T. W. Hamilton, B. P. Aragon, R. J. Shul and C. G. Willison, Journal of Vacuum Science & Technology a-Vacuum Surfaces and Films **20,** 873-886 (2002).

11 M. D. Shirk and P. A. Molian, Journal of Laser Applications **10,** 18-28 (1998).

12 A. V. Simakin, G. A. Shafeev and E. N. Loubnin, Applied Surface Science **154,** 405-410 (2000).

13 S. J. Shaw, W. P. Schiffers, T. P. Gentry and D. C. Emmony, J. Phys. D: Appl. Phys **32,** 1612-1617 (1999).

14 O. Yavas, A. Schilling, J. Bischof, J. Boneberg and P. Leiderer, Applied Physics A **64,** 331-339 (1997).

15 A. V. Simakin, E. N. Loubnin and G. A. Shafeev, Applied Physics a-Materials Science & Processing **69,** S267-S269 (1999).

16 Y. F. Lu, S. M. Huang, C. H. A. Huan and X. F. Luo, Applied Physics a-Materials Science & Processing **68,** 647-651 (1999).

17 G. W. Yang and J. B. Wang, Applied Physics a-Materials Science & Processing **71,** 343-344 (2000).

18 S. I. Dolgaev, A. V. Simakin, V. V. Voronov and G. A. Shafeev, Applied Surface Science **186,** 546-551 (2002).

19 J. B. Wang, G. W. Yang, C. Y. Zhang, X. L. Zhong and Z. H. A. Ren, Chemical Physics Letters **367,** 10-14 (2003).

20 G. W. Yang, J. B. Wang and Q. X. Liu, Journal of Physics: Condensed Matter **10,** 7923-7927 (1998).

21 J. B. Wang and G. W. Yang, Journal of Physics: Condensed Matter **11,** 7089-7094 (1999).

22 J. B. Wang, C. Y. Zhang, X. L. Zhong and G. W. Yang, Chemical Physics Letters **361,** 86-90 (2002).

23 P. W. May, Philosophical Transactions of the Royal Society of London Series a-Mathematical Physical and Engineering Sciences **358,** 473-495 (2000).